

Heisenberg model for the square-planar lattice and fragments

T. P. Živković, B. L. Sandleback, T. G. Schmalz, and D. J. Klein

Theoretical Chemical Physics Group, Texas A&M University at Galveston, Galveston, Texas 77553-1675

(Received 6 April 1989; revised manuscript received 21 July 1989)

Finite-fragment computations for the ground state of the isotropic spin- $\frac{1}{2}$ Heisenberg model for the square-planar lattice are made. Both the exact ground-state and the (severe form of the) resonating-valence-bond ansatz are considered and compared. Energy extrapolations to infinite strips and then the infinite lattice are attempted. A novel real-space renormalization for the ground state is also carried out, and finally the possibility of single-soliton excitations is considered. The short-range ansatz is found to give only a modest improvement beyond a simple Néel state and to be unstable to disproportionation into well-separated single spins.

I. INTRODUCTION

The antiferromagnetically signed Heisenberg spin Hamiltonian is an explicitly correlated many-body model of use in describing magnetic phenomena. Though of general interest, the nature of the ground-state and low-lying excitations is not fully known for arbitrary arrangements of spin-carrying sites. Anderson¹ has suggested that this model may be of relevance for understanding the high-temperature superconductivity of the ceramic perovskites, which apparently consist of infinite two-dimensional square-planar arrays of active copper atoms, each with a single active orbital. Anderson¹ has proposed that the ground state of such a square-planar layer might be accurately described by a "resonating-valence-bond" (RVB) wave function, i.e., by a superposition of wave functions in which each site is singlet spin paired to one other site.

In this paper we investigate the ground state of the Heisenberg model for fragments cut from the square-planar lattice, for infinite-length strips, and finally for the lattice itself. We compare the exact energy estimates to energies evaluated from a rather severe RVB-type approximate wave function, the so-called "short-range" RVB wave function² in which spin pairings are restricted to nearest-neighbor pairs of sites only. These nearest-neighbor spin-paired configurations are termed "Kekulé structures" in chemistry. For reasonably small finite fragments, numerically exact ground-state energies can be obtained via full configuration interaction (CI) over the space of homopolar singlet states. One efficient scheme for performing such calculations, used here, is a graphical unitary-group approach,³ which permits calculations on fragments of up to about 20 sites on ordinary computers, with 24 or 26 sites the limit on supercomputers. We restrict our attention to fragments which are bipartitionable into two equicardinal sets such that sites in one set are bonded only to sites in the other. In this case the ground state is known to be a singlet.⁴ In this case also, the energy for the simplest nearest-neighbor RVB ansatz of Pauling and Wheland⁵ can be calculated via matrix element formulas developed some time ago by Pauling,⁶ though for polymeric (long strip) species this ap-

proach can be profitably refined.⁷

The computational results on finite fragments may be utilized to make estimates for extended systems. One approach taken in Secs. III and IV is first to make ground-state energy extrapolations as a function of strip length to yield estimates for infinite strips of fixed width, and second to extrapolate as a function of strip width to yield an estimate for the two-dimensional lattice. This approach helps to disentangle the effects of a novel long-range order, which may be of physical relevance. The approach of Sec. V utilizes the results of finite-fragment computations to effect a real-space renormalization transformation modified from earlier ones^{8,9} which then also leads to a good ground-state energy estimate for the infinite lattice. Finally, Sec. VI uses finite-fragment results to make some estimates of solitonic excitations within the VB picture.

II. COMPUTATIONS ON LATTICE FRAGMENTS

We consider rectangular fragments of width w and length L cut from the square-planar lattice. We take the Hamiltonian as

$$H = J \sum_{i \sim j} 2\mathbf{s}_i \cdot \mathbf{s}_j, \quad (2.1)$$

where J is the (positive) exchange parameter, \mathbf{s}_i and \mathbf{s}_j are site spin operators, and the sum goes over nearest neighbors. With the above Hamiltonian the energy of a single nearest-neighbor spin pairing (i.e., Kekulé structure) is $-3JN/4$ where $N = wL$ is the number of sites. If this value is subtracted from the computed energy of a system, the difference represents the extra stabilization due to interactions among the spin pairings. Such energy differences are often termed resonance energies in the chemical literature.⁵

The exact ground-state energy of each fragment is obtained by full CI using the whole singlet-space matrix representation on the Gelfand-Zetlin basis, along with a modified Davidson algorithm¹⁰ to extract the lowest eigenvalue. The RVB ansatz is taken as

$$|\Psi_{\text{RVB}}\rangle = \sum_K |K\rangle \quad (2.2)$$

TABLE I. Energy per site for fragments of the square-planar lattice (units of J).

w	L	$K(w \times L)$	$\kappa(w \times L) - 0.75$	E^{RVB}	E^{exact}
2	2	2	-1.010	-1.000 000	-1.000 000
2	3	3	-1.025	-1.022 727	-1.043 128
2	4	5	-1.052	-1.048 469	-1.073 267
2	5	8	-1.062	-1.060 448	-1.089 342
2	6	13	-1.071	-1.069 168	-1.100 579
2	7	21	-1.076	-1.075 301	-1.108 475
2	8	34	-1.081	-1.079 876	-1.114 434
2	9	55	-1.084	-1.083 465	-1.119 059
2	10	89	-1.087	-1.086 317	-1.122 762
2	11	144	-1.089	-1.088 661	
3	4	11	-1.050	-1.051 948	-1.115 280
3	6	41	-1.059	-1.062 361	-1.142 613
3	8	153	-1.064	-1.067 526	
3	10	571	-1.067	-1.070 617	
3	12	2131	-1.069	-1.072 675	
4	4	36	-1.086	-1.087 456	-1.148 651
4	5	95	-1.092	-1.094 385	-1.165 157
4	6	281	-1.102	-1.105 128	
4	7	781	-1.107	-1.110 034	
4	8	2245	-1.112	-1.114 965	
4	9	6336	-1.115	-1.118 224	
5	6	1183	-1.104	-1.107 154	
6	6	6728	-1.117	-1.120 581	

with $|K\rangle$ a nearest-neighbor spin-pairing structure (Kekulé structure) with phases chosen in the natural conventional manner. Of course, we are restricted to fragments with w or L or both even, in order to admit a dimer covering. The matrix elements of H in the basis of configurations $|K\rangle$, as well as the overlaps $\langle K|K'\rangle$, are evaluated by graphical techniques⁶ using a slightly modified version of a BORT (Ref. 11) program.

The exact and RVB per-site resonance energies for the fragments which we have treated are reported in Table I. Also shown is a per-site measure of the number of Kekulé structures

$$\kappa(w \times L) = -1.5 \frac{\ln K(w \times L)}{wL}, \quad (2.3)$$

where $K(w \times L)$ is the total number of Kekulé structures for the $w \times L$ fragment and the constant 1.5 has been included to provide a rough scaling to approximate per-site resonance energies (in units of J). Then $\kappa(w \times L)$ plus the energy (-0.75) per site of a single Kekulé structure should give an estimate of the energy per site for the short-range RVB ansatz.

Inspection of the data in Table I produces several observations. First, the per-site energies in general increase with increasing fragment size, although the shape of the fragment can have a significant effect. Second, both the RVB energies and Kekulé counts qualitatively show the same trends as the exact energies, though the RVB results become poorer as the fragments become larger. This is consistent with earlier work¹² indicating that the Kekulé structures form a good basis at low average coordination number, but become less good as the average coordination number increases above 3. Finally, along

sequences of fixed (even) width w , there is a pronounced even-odd fluctuation with length. We will examine this point in more detail in the next section as we consider the approach to the infinite lattice.

III. EXTRAPOLATION TO LONG STRIPS

A. RVB wave function

We consider first the extrapolation of fragment data for fragments of fixed width but increasing length. Fortunately, for the RVB calculations we can obtain considerable insight into the approach to this limit by examining the transfer matrix formulation of the problem.¹³ For $w=2$, the transfer matrix turns out to be only 3×3 , and the energy of a fragment of any length can be expressed completely in terms of the three eigenvalues and associated eigenvectors of the transfer matrix.¹³ This analysis shows that the overlap of the RVB wave function with itself can be written as

$$\langle \Psi_{\text{RVB}} | \Psi_{\text{RVB}} \rangle = \sum_{i \geq 1} (A_w^{(i)} L + B_w^{(i)}) \lambda_i^L, \quad (3.1)$$

where the A 's and B 's are constants determined by the eigenvectors (depending only on w), and the λ_i are the eigenvalues of the transfer matrix. Similarly, the matrix element of the Hamiltonian can be written as

$$\langle \Psi_{\text{RVB}} | H | \Psi_{\text{RVB}} \rangle = J \left[\tilde{A}_w L + \tilde{B}_w + \sum_{i > 1} (C_w^{(i)} L + D_w^{(i)}) \rho_i^L \right] \lambda_1^L, \quad (3.2)$$

where \tilde{A}_w , \tilde{B}_w and the C 's and D 's are constants and $\rho_i \equiv \lambda_i/\lambda_1$ with λ_1 being the maximum-magnitude eigenvalue of the transfer matrix. The RVB estimate of the ground-state energy is given simply by the ratio of (3.2) to (3.1). Clearly, as L increases only the contribution from the largest eigenvalue survives, and the energy per site in units of J is given by $E_w = \tilde{A}_w/wA_w^{(1)} = -1.112058$ to computer accuracy.

Equation (3.2) rationalizes the even-odd fluctuation in the approach to the limit. As discussed below, for odd-width strips all eigenvalues of the transfer matrix come in \pm pairs. For even-width strips the two maximum modulus eigenvalues do not have to be equal, but in all cases which we have examined the second largest eigenvalue in magnitude is opposite in sign to the first, so that the largest term in the sum in (3.2) changes sign as L is even or odd.

The term B_w in (3.2) accounts for the contributions of the strip ends. It could be eliminated by imposing cyclic boundary conditions, but this increases the dimension of the transfer matrix and increases the importance of the exponential terms in the sum in (3.2), so that we find that we can extrapolate more accurately from data for fragments without cyclic boundary conditions. When cyclic boundary conditions are not used, the magnitude of the sum of all the exponential terms in the expression for the energy for width $w=2$ has dropped to 0.0068 at $L=4$ and is less than 1×10^{-4} for $L \geq 6$. By contrast, for strips with cyclic boundary conditions in the length direction (which requires L even unless the strips are allowed to "twist"), the exponential corrections are much larger: 0.532, 0.190, 0.057, and 0.016 for $L=4, 6, 8,$ and 10 .

For width 3 strips the transfer matrix is formally 14×14 , but as indicated above, all eigenvalues come in \pm pairs, so that in fact a 7×7 matrix suffices to determine the magnitudes. Thus, for odd-length strips, all \pm contributions cancel exactly leading to zero resonance energy as must happen since there are no Kekulé structures possible. For even-length strips the contributions of each positive eigenvalue are just doubled, and since the first term in the sum in (3.2) is really the third largest eigenvalue, the convergence to the limit is faster. For $w=3$ we obtain $E_w = \tilde{A}_w/wA_w^{(1)} = -1.082968$.

For $w=4$ the transfer matrix is 22×22 and thereafter their sizes continue to rapidly increase, roughly $\sim 3^w$, so that their construction becomes difficult. We have therefore estimated the per site energy of the infinite strips by extrapolation, using the forms of (3.2) and (3.1) as guides. For odd widths we have simply plotted per-site energies versus $1/L$, ignoring all exponential terms, and taken E_w from the $1/L=0$ intercept. For even w , the data have been fit to the equation

$$E(w \times L)/J = E_w L + \beta_w + (\gamma_w L + \delta_w) \rho_w^L, \quad (3.3)$$

where the term proportional to ρ_w^L with $\rho_w < 0$ accounts for the leading, even-odd dependent, term in the sum in (3.2). These extrapolated estimates are collected in Table II.

TABLE II. Energy per site for infinite-length strips of the square-planar lattice (units of J).

w	E^{RVB}	E^{exact}
1	-0.750 000	-0.886 294
2	-1.112 058	-1.156
3	-1.082 968	-1.188
4	-1.146	-1.236
5	-1.133	
6	-1.161	

B. Exact wave function

For the exact results we have fewer data points to work with and we do not have a transfer matrix available to guide our extrapolation. However, if the RVB approximation is a tolerable approximation to the exact wave function, it seems reasonable to assume that the functional dependence of the energy is not too different from that discussed above. We have therefore adopted the same procedure for extrapolating the exact energies as was used for the RVB energies. For $w=3$ the fragment energies were just plotted against $1/L$, while for $w=2$ and $w=4$ Eq. (3.3) was used. To get the five data points needed at $w=4$ we have added the value for a 4×1 chain ($E = -0.982051$). These extrapolated results are also presented in Table II. The value for the $1 \times \infty$ chain is exactly known from Hulthén.¹⁴

C. Effects of long-range order

It is clear that even for infinite strips there is a fluctuation in the per site energy depending on whether the width is even or odd. The difference between the CI and RVB results also depends on strip width. To a certain extent the fluctuations correlate with the fluctuations in the per-site Kekulé-structure counts $\kappa(w \times \infty)$, and these in turn correlate with the long-range spin-pairing order described in the accompanying paper. For instance, for a

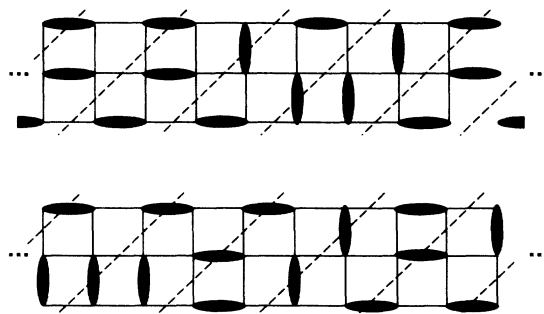


FIG. 1. Example dimer coverings (or Kekulé structures) on portions of two very long width-3 strips, with dashed lines indicating divisions between unit cells. In the first and second cases here there are, respectively, one and two dimers (or spin pairings) crossing each unit-cell boundary.

very long $w=3$ strip we display two Kekulé structures in Fig. 1. In the first and second of these structures one sees, respectively, $Q=1$ and $Q=2$ spin pairings across each of the dashed lines indicating a position along the strip. Indeed, this number Q of spin pairings remains fixed no matter how either Kekulé structure is extended and so these two counts identify two different long-range-order classes. Generally if one restricts counts $K_Q(w \times \infty)$ to Kekulé structures with a fixed Q , then $K_Q(w \times \infty)$ should vary as an even function of $(Q/w - 1/2)$ with a maximum at $Q/w = 1/2$. This is explicitly illustrated for $K_Q(w \times \infty)$ in an accompanying paper for the $w \rightarrow \infty$ limit. Now it may be seen that our even-width strips deal with $Q/w = 1/2$ while the odd-width ones have $Q/w = 1/2 - 1/2w$. Thus odd-width strips have fewer Kekulé structures per site (especially for smaller w) so that less configuration mixing among these Kekulé structures occurs and so that there is a lesser lowering of the ground-state energy. Of the even-width strips the smallest might be anticipated to be best described by the RVB ansatz since there the associated lower coordination numbers imply the alternative Néel-state picture is less accurate. These expectations are seen to be in conformity with the results of Table II, and other results have been¹² similarly interpreted.

As long as cyclic boundary conditions are not used, only the Q values consistent with the strip ends occur, and here we have chosen these ends to be consistent with Q/w as near to the maximum at $1/2$ as possible. However, if cyclic boundary conditions are employed, then all Q values occur (for finite lengths), and as indicated previously, the convergence to the infinite (uncoupled) limit is less rapid.

IV. EXTRAPOLATION TO THE SQUARE-PLANAR LATTICE

A. RVB wave function

Next, extrapolation of the E_w of the preceding section to the (infinite-width) square-planar lattice may be made. Unlike the length extrapolation where the corrections other than for the ends are expected to damp exponentially, we expect the width corrections to decay as reciprocal powers. We therefore presume an asymptotic form

$$E_w \cong \varepsilon w + a + b/w, \quad w \rightarrow \infty \quad (4.1)$$

with ε the bulk per site energy, and a , the edge term, the same for all strips, but with b different for odd- and even-width strips (as indicated by the long-range-order considerations of the preceding section). This form of (4.1) is found in analytic transfer-matrix enumerations for Kekulé structures on finite-width strips, as described in the accompanying paper. Since this enumeration itself can be viewed as arising from an orthogonalized version of the short-range RVB description, (4.1) is suggested for the present RVB energies. When we fit the RVB data for $w=1,3,5$ and then that for $w=2,4,6$ to (4.1) we obtain, respectively, $\varepsilon = -1.1977$ and $\varepsilon = -1.1965$. The agreement is gratifying, and we take the mean, $\varepsilon = -1.197$, as our best estimate of the short-range RVB energy of the square-planar lattice, but the small number of data points used in both the width and some of the length extrapolations suggests an error bar of about ± 0.010 . We have collected our own and various other estimates of the square-planar lattice energy in Table III.

TABLE III. Per-site ground-state energy estimates for the square-planar lattice.

Method	Reference	ε
Single Kekulé state		-0.7500
Néel state		-1.0000
Fragment extrapolation—short-range RVB	This work	-1.197±0.01
Fragment extrapolation—diagonalization in Kekulé basis	15	-1.200±0.01
Monte Carlo short-range RVB	16	-1.208±0.0008
Variational spin-wave-like	23	-1.286
Antiferromagnetic spin wave	25	-1.290
Fragment extrapolation—exact diagonalization	15	-1.302±0.01
Fragment extrapolation—exact diagonalization	20	-1.31±0.01
Approximate variational	22	-1.312
Approximate variational	24	-1.316
Monte Carlo variational	17	-1.3276
Renormalization	This work	-1.332
Second-order Néel state		-1.3333
Sixth-order Néel state	26	-1.3345
Extrapolated infinite-order Néel state	21	-1.336±0.004
Monte Carlo—long-range RVB	16	-1.3364±0.0008
Fragment extrapolation—exact diagonalization	This work	-1.337±0.015
Monte Carlo—Néel type	16	-1.3376±0.0008
Monte Carlo—extrapolation	18	-1.340±0.004
Monte Carlo—extrapolation	19	-1.3448±0.001

Our RVB result should be an upper bound to the exact energy—evidently not too close a one. It apparently, however, is a very close upper bound to the energy determined by diagonalization in the space of Kekulé structures, which has been estimated by extrapolation.¹⁵ The value of Liang *et al.*¹⁶ indicates that the error entailed in equally weighting all Kekulé structures is even smaller, since their Monte Carlo calculation gives a presumably more accurate slightly lower estimate of what the extrapolated limit should be.

B. Exact wave function

Since for the exact energy estimates we have only four data points, we have used (4.1) along with the assumption that ε and a are the same for odd and even width to determine the four parameters ε , a , b^{odd} , b^{even} . This gives $\varepsilon = -1.337$ for the exact per-site energy of the lattice, but here even larger error bars of about ± 0.015 seem prudent. This value is also included in Table III.

This estimate seems to be in reasonable agreement with most other entries in Table III. In particular it is slightly lower than the variational approach of Huse and Elser¹⁷ and the best RVB-type wave function of Liang *et al.*¹⁶ It is slightly higher than the best Néel state-based wave function of Liang *et al.*¹⁶ and the Monte Carlo extrapolation of Reger and Young.¹⁸ Our estimate is significantly above the estimate of Barnes and Swanson¹⁹ obtained by extrapolation of Monte Carlo results for various fragments (up to 40 by 40). Indeed we are about seven of their standard deviations above their estimate, but it may be noted that for the 4 by 4 fragment (with cyclic boundary conditions) they are about three standard deviations below the (accurately numerically determined) exact energy. On the other hand, our estimate is notably lower than two^{15,20} earlier extrapolations of finite-fragment results, but Huse²¹ has argued that these earlier results are faulty in making an incorrect assumption as to the N dependence of the finite-fragment correction. Several other^{22–24} variationally based estimates give values somewhat higher, as presumably they should. Also included is the antiferromagnetic spin-wave result.²⁵ Néel-state perturbation expansion^{21,26} seems to converge quite rapidly to a reasonably accurate result, close to the long-range RVB result. It is still not clear whether the exact wave function should fall into the universality class of the Néel state or of the RVB wave function, associated to different types of long-range order.

V. RENORMALIZATION ESTIMATE

Before considering the results of Sec. IV in more detail, we make an alternative estimate of the lattice energy. Finite-fragment data may be renormalized to estimate the lattice energy via an approximate real-space renormalization transformation. For the present square-planar problem 3×3 blocks are renormalized to single sites in the new transformed Hamiltonian

$$H^{(1)} = \sum_{i'} A^{(1)} + \sum_{i' \sim j'} (B^{(1)} + J^{(1)} 2\mathbf{s}_{i'} \cdot \mathbf{s}_{j'}), \quad (5.1)$$

where $\mathbf{s}_{k'}$ is the spin operator for block k' , the first sum is over blocks, and the second sum is over adjoining blocks.

Iteration of the transformation yields a sequence $H^{(1)}$, $H^{(2)}$, \dots of renormalized Hamiltonians. The associated $A^{(n)}$, $B^{(n)}$, and $J^{(n)}$ simply effect shifts and rescalings, so that there are three n -independent parameters α , β , and γ , such that

$$\begin{aligned} A^{(n)} &= 9A^{(n-1)} + 12B^{(n-1)} + \alpha J^{(n-1)}, \\ B^{(n)} &= 3B^{(n-1)} + \beta J^{(n-1)}, \\ J^{(n)} &= \gamma J^{(n-1)}. \end{aligned} \quad (5.2)$$

Here the factors 9 and 12 for $A^{(n-1)}$ and $B^{(n-1)}$ in the first equation arise in counting the number of sites and bonds internal to a block, while in the second equation the factor of 3 for $B^{(n-1)}$ arises in counting the number of bonds between two adjoining blocks. Then

$$\begin{aligned} J^{(n)} &= \gamma^n J^{(0)}, \\ B^{(n)} &\rightarrow 3^n \left[B^{(0)} + \frac{\beta}{3-\gamma} J^{(0)} \right], \\ A^{(n)} &\rightarrow 9^n \left[A^{(0)} + 2B^{(0)} + \frac{\alpha + 2\beta}{9-\gamma} J^{(0)} \right], \end{aligned} \quad (5.3)$$

so that (with $A^{(0)} = B^{(0)} = 0$, $J^{(0)} = J$, which is appropriate for the spin Hamiltonian of Eq. (2.1)) the large-limit per-site ground-state energy is

$$\varepsilon = \lim_{n \rightarrow \infty} 9^{-n} A^{(n)} = \left[\frac{\alpha + 2\beta}{9-\gamma} \right] J. \quad (5.4)$$

One method now used several times to determine the renormalization transformations is via a first-order degenerate perturbation-theoretic development.^{8,9} Here we obtain the renormalization parameters α, β, γ in an alternative way via a cluster-expansion technique which uses finite-fragment results. That is, numerically exact CI computations are carried out for the 3×3 and 3×6 fragments (consisting of one and two blocks), and the exact renormalization parameters are determined to transform these to 1- and 2-site renormalized models, H_1 and H_{12} . Thence H_1 for block 1 (and H_2 for a second single block 2) is simply a scalar giving the doublet ground-state energy $E_D(3 \times 3)$ for the 3×3 block,

$$E_D(3 \times 3) = A^{(1)}. \quad (5.5)$$

Next the renormalized two-block Hamiltonian H_{12} is to give the lowest singlet and triplet energies for the 3×6 fragment

$$\begin{aligned} E_S(3 \times 6) &= 2A^{(1)} + B^{(1)} - 3/2J^{(1)}, \\ E_T(3 \times 6) &= 2A^{(1)} + B^{(1)} + 1/2J^{(1)}. \end{aligned} \quad (5.6)$$

Thence (5.5) and (5.6) may be inverted to obtain $A^{(1)}$, $B^{(1)}$, $J^{(1)}$, following which (5.2) with $n = 1$ may be inverted to obtain α, β, γ , and finally with (5.4) one obtains

$$\varepsilon = \frac{E_S(3 \times 6) + 3E_T(3 \times 6) - 6E_D(3 \times 3)}{18 - E_T(3 \times 6) + E_S(3 \times 6)}. \quad (5.7)$$

Using the calculated fragment energies $E_D(3 \times 3) \cong -9.498\,655$, $E_S(3 \times 6) \cong -20.567\,036$, $E_T(3 \times 6) \cong -19.790\,718$, gives $\varepsilon \cong -1.332$, in quite reasonable agreement with the extrapolated result of -1.337 from the last section. The result is notably better than that^{27,9} of $\varepsilon \cong -1.1184$ from the first-order degenerate perturbation treatment (which also gives a rigorous upper bound). The superiority of the cluster-expansion technique we believe is not fortuitous, but, e.g., is also found for the linear chain where the first-order perturbation and our three-to-one cluster-expansion methods give $\varepsilon \cong -0.7826$ and $\varepsilon \cong -0.8969$ as compared to the exact result, $\varepsilon \cong -0.886\,294$, of Hulthén.¹⁴

VI. SOLITONIC EXCITED STATES

Finite-fragment computations may also be organized to test for the possibility of solitonic excited states. This is most simply approached within the RVB framework, where the excited-state configurations are to have all sites (singlet) spin paired to nearest neighbors except for a single pair of sites which are well separated from one another. This criterion of well-separatedness may be imposed simply by considering strips with an odd number of sites. Thence a typical RVB configuration $|iC\rangle$ has site i unpaired, with a nearest-neighbor pairing pattern for all remaining sites. The short-range RVB *ansatz* then is

$$|\Psi_{\text{RVB}}\rangle = \sum_i \sum_C^* |iC\rangle, \quad (6.1)$$

$$\Delta(3 \times L) = \begin{cases} \frac{1}{2}[E_D(3 \times L + 1) + E_D(3 \times L - 1)] - E_S(3 \times L), & L \text{ even} \\ E_D(3 \times L) - \frac{1}{2}[E_S(3 \times L + 1) + E_S(3 \times L - 1)], & L \text{ odd} \end{cases} \quad (6.2)$$

The doublet energies of both RVB and exact wave functions for the various $3 \times L$, $L = \text{odd}$, fragments were computed, and the excitation energy estimates obtained therefrom are reported in Table IV. These results for the exact and short-range RVB wave functions differ marked-

TABLE IV. Excitation energy estimates.

L	$\Delta(3 \times L)$	
	Exact	RVB
2	+0.5094	+0.5000
3	+0.3224	+0.1071
4	+0.2464	-0.1131
5	+0.1999	-0.3272
6		-0.4757
7		-0.6247
8		-0.7344
9		-0.8442
10		-0.9269
11		-1.0097

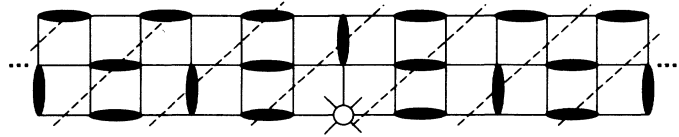


FIG. 2. A depiction of a typical structure $|iC\rangle$ with a single unpaired site on a width-3 strip. There are, respectively, one or two dimers crossing unit-cell boundaries to the left or right of the unpaired site.

where the i sum is over the sublattice with an excess of one site. The relevant matrix elements were again developed by Pauling.⁶

An important constraint arises if Ψ_{RVB} of (6.1) is to be a reasonable ansatz. Note that for a configuration $|iC\rangle$, as in Fig. 2, the long-range-order parameter Q changes by 1 in crossing past the site i of the unpaired spin. So if the Q and $Q \pm 1$ phases are of different energies (i.e., are non-degenerate), then the amount of higher-energy phase should be minimized, with the unpaired site i becoming localized near one end of the strip. Such nondegeneracy arises with the even-width w strips, so that a solitonic description as in (6.1) would not be reasonable (except perhaps if w were very large). But for odd-width strips the two phases are degenerate with $Q = (w \pm 1)/2$, so that Ψ_{RVB} of (6.1) is a reasonable candidate wave function.

With note of the ideas in the preceding paragraphs we focus on the $3 \times L$ strips. An excitation energy estimate can be obtained as

ly. For the exact wave function the $\Delta(3 \times L)$ are positive and when plotted versus $1/L$ reasonably extrapolate in a linear fashion to near 0 as $L \rightarrow \infty$. In fact, this is what is expected theoremtically.²⁸

The computed excitation energies for the short-range RVB ansatz deserve special note. First, they are *negative*, indicating that this RVB ansatz is unstable to disproportionation into spins that are not locally paired. That is, a more favorable candidate would have a nonzero concentration of such spins not locally paired. Extrapolation of the RVB finite-fragment results of Table IV turns out to be a more delicate matter: The linear region in a plot of $\Delta_{\text{RVB}}(3 \times L)$ versus $1/L$ evidently is not reached until L exceeds the values of Table IV. (A similar behavior is observed for $w = 1$, where the RVB results are readily obtained for arbitrary length L .) Nevertheless the $\Delta_{\text{RVB}}(3 \times L)$ seem clearly to decrease monotonically as L increases; they seem to approach a value of about -2 .

Of course the width $w = 3$ strip is not the full square-planar lattice. Moreover the $w = 3$ ground-state against

which the excitations are gauged have $q/w = 1/3$, rather than the presumably more energetically preferred $q/w = 1/2$, such as would occur for the full lattice. Thus the excitations should be more costly for the full lattice, but as we estimate it, not enough to prevent disproportionation. That is, from Table II of Sec. III the ground-state energy per site for the full lattice is estimated to be about 0.25 lower than for the $w = 3$ strip, so that the full-lattice excitation energy is still estimated to be strongly negative. We conclude that the actual ground-state wave function for the square-planar nearest-neighbor $s = 1/2$ Heisenberg model is not well described by the *short-range* RVB ansatz. Perhaps a Néel-state description may be better—surely so far as the associated energy estimate is concerned.

VII. CONCLUSION

We have investigated both the short-range RVB ansatz and the exact ground state for strips cut from the square-planar lattice and attempted extrapolations to the full lattice. Accurate numerical estimates have been given for both types of energies for various strip widths and for the full lattice. This work finds the short-range RVB energy for the width $w = 2$ strip to be quite reasonable, but especially for wider strips and the full-lattice Néel-state-based energies appear to be much superior. Further evidence in support of this is found in our study of excitations in sec. VI, where we find the short-range RVB wave function unstable to disproportionation into well-separated spins not locally paired. This can destroy the type of long-range spin-pairing order we have noted to be associated to short-range RVB descriptions and thence allows the possibility of the (otherwise inconsistent) usual Néel-state ordering. That the exact wave function should fall into the universality class of the Néel-state is not at all clear though, because of the evident high accuracy of the long-range RVB energy.¹⁶

The possibility that the short-range RVB model provides a reasonable description under other circumstances remains. First if on the square-planar lattice antiferromagnetically-signed exchange interactions $2s_i \cdot s_j$

between diagonally situated next-nearest neighbors are allowed, then Néel-state ordering is “frustrated” while the energy for single Kekulé structures remains unchanged. Anderson¹ has mentioned such interactions as a possible stabilizing influence for the RVB description. However, in deriving effective spin Hamiltonians from the Hubbard model one may note that there arise (in the same order) quartic spin interactions around size-4 rings which destabilize the RVB description²⁹—indeed, in chemistry, this destabilization is associated to Hückel’s $4n$ -rule. Corrections to the simple Heisenberg model then come into question. A further crucial modification concerns the inclusion of an additional concentration of electrons (or holes). In this case the RVB ansatz modifies to appear much like that of the excitations of Sec. VI but where now the singular sites have double (or empty) electron occupancy. The relevant matrix elements are somewhat like those of Sec. VI, so that the negative excitation energies found there indicate that the inclusion of such charge-carrying single sites should enhance the stability of the short-range RVB description. At the same time this would destabilize Néel-state descriptions. Overall this is possibly very pertinent since experimentally there is antiferromagnetic Néel-state ordering for the stoichiometric case, while superconduction occurs for nonstoichiometric species for which one could include a nonzero concentration of double (or empty) electron occupancies on the sites. Finally if the coordination number is lowered (while still allowing many Kekulé structures), the short-range RVB ansatz is enhanced as we have argued before.¹² Indeed the present conclusions are quite consistent with this earlier stated view.

Note added in proof. What seems to us the best ground-state energy estimate (see Table III) so far is -1.33836 ± 0.0002 obtained by J. Carlson, Phys. Rev. B **40**, 846 (1989) via a Monte Carlo extrapolation.

ACKNOWLEDGMENTS

This research was supported by The Welch Foundation of Houston, Texas, and an equipment grant from AT&T Corporation.

¹P. W. Anderson, Science **235**, 1196 (1987).

²D. S. Rokhsar and S. A. Kivelson, Phys. Rev. B **61**, 2376 (1988).

³S. A. Alexander and T. G. Schmalz, J. Am. Chem. Soc. **109**, 6933 (1987).

⁴E. H. Lieb and D. C. Mattis, J. Math. Phys. **3**, 749 (1962).

⁵L. Pauling and G. W. Wheland, J. Chem. Phys. **1**, 362 (1933).

⁶L. Pauling, J. Chem. Phys. **1**, 280 (1933).

⁷D. J. Klein, T. G. Schmalz, G. E. Hite, A. Metropoulos, and W. A. Seitz, Chem. Phys. Lett. **120**, 367 (1985).

⁸H. P. van de Braak, W. J. Caspers, F. W. Wiegel, and M. W. M. Willamse, J. Stat. Phys. **18**, 577 (1978); J. N. Fields, Phys. Rev. B **19**, 2637 (1979); H. W. J. Blöte, J. C. Bonner, and J. N. Fields, J. Magn. Magn. Mater. **15-18**, 405 (1980); P. M. van den Broek, J. Phys. C **13**, 5423 (1980); W. J. Caspers, Phys. Rep. **63**, 224 (1980).

⁹D. C. Mattis and C. Y. Pan, Phys. Rev. Lett. **61**, 463 (1988); **61**, 2279 (1988).

¹⁰J. Cullum and R. A. Willoughby, J. Comp. Phys. **44**, 329 (1981); E. R. Davidson, *ibid.* **17**, 87 (1975).

¹¹T. P. Živković, J. Mol. Struct. **185**, 169 (1989).

¹²D. J. Klein, S. A. Alexander, W. A. Seitz, T. G. Schmalz, and G. E. Hite, Theor. Chim. Acta **69**, 393 (1986).

¹³D. J. Klein, G. E. Hite, and T. G. Schmalz, J. Comp. Chem. **7**, 443 (1986); G. E. Hite, A. Metropoulos, D. J. Klein, T. G. Schmalz, and W. A. Seitz, Theor. Chim. Acta **69**, 369 (1986).

¹⁴L. Hulthén, Ark. Mat. Astron. Fys. **26A**, 1 (1938).

¹⁵M. O. Johnson and K. R. Subbaswamy, Phys. Rev. B **37**, 9390 (1988).

¹⁶S. Liang, B. Doucot, and P. W. Anderson, Phys. Rev. Lett. **61**, 365 (1988).

¹⁷D. A. Huse and V. Elser, Phys. Rev. Lett. **60**, 2531 (1988).

¹⁸J. D. Reger and A. P. Young, Phys. Rev. B **37**, 5978 (1988).

¹⁹T. Barnes and E. S. Swanson, Phys. Rev. Lett. **B 37**, 9405 (1988).

²⁰J. Oitmaa and D. D. Betts, Can. J. Phys. **56**, 897 (1978).

- ²¹D. A. Huse, Phys. Rev. B **37**, 2380 (1988).
- ²²W. Marshall, Proc. R. Soc. London, Ser. A **232**, 48 (1955).
- ²³T. Oguchi, J. Phys. Chem. Solids **24**, 1649 (1963).
- ²⁴R. Bartowski, Phys. Rev. B **5**, 4536 (1972).
- ²⁵P. W. Anderson, Phys. Rev. **86**, 694 (1952); R. Kubo *ibid.* **87**, 568 (1952).
- ²⁶M. Parrinello, M. Scire, and T. Aria, Lett. Nuovo Cimento **6**, 138 (1973).
- ²⁷J. S. Yedidia, Phys. Rev. Lett. **61**, 2278 (1988).
- ²⁸E. H. Lieb, T. D. Schultz, and D. C. Mattis, Ann. Phys. (N.Y.) **16**, 407 (1961); I. Affleck, Phys. Rev. B **37**, 5186 (1988).
- ²⁹R. D. Poshusta, T. G. Schmalz, and D. J. Klein, Mol. Phys. **66**, 317 (1989).